Proceedings of 20th International Congress on Acoustics, ICA 2010

23-27 August 2010, Sydney, Australia

Vibro-acoustic behaviour of micro-perforated plate for sound absorption performance

Toshimitsu Tanaka (1), Kusakari Tatsuhiro (1) and Tsugihashi Kazuki (2)

(1) Seikei University, Tokyo, Japan
(2) Kobe Steel Co.Ltd., Kobe, Japan

PACS: 43.55.Ev Sound absorption propeties of materials: Theory and measurement of sound absorption coefficient

43.40.At Experimental and theoretical studies of vibrating systems

ABSTRACT

As a new sound absorption material, micro-perforated aluminium thin plate has been developed, which is tough for water, oil, or heat. But thin elastic plate is easily vibrated by sound pressure. And the vibration affects the performance of sound absorption. We experimented to make clear the relation between the coefficient of sound absorption and the vibration of micro-perforated plate (MPP). Resonant frequencyies and vibration modes of micro-perforated thin aluminum plate were observed by using the scanning laser Doppler vibrometer, and the sound absorption coefficient of that plate was measured by two- microphone method. We found that the sound absorption performance is affected by resonant vibration modes, and that the remarkable depression of sound absorption performance was caused by the special vibration mode in which the phase of particle velocity of air and vibration velocity of the elastic plate became same in main area of the plate. We also found that adding damping is effective to improve the local depression of the sound absorption coefficient of micro-perforated elastic plate.

1. INTRODUCTION

A new type of sound absorption material, micro-perforated aluminum thin plate or foil has been developped[1]. It has advantage to be tough for water, heat-registance and strength. It also has advantage for environmental problem of CO_2 , if it is light and can be made of a recyclable resource. But the stiffness of thin plate or foil is generally low, so it is easily vibrated by sound pressure. And it is considered that it's vibration affects the performance of sound absorption power to decrease the coefficient of sound absorption. Therefore it is desirable for us to understand the relation between the vibration behaviour and the performance of sound absorption and how to recover the sound absorption power for rational design of sound absorbing panels.

Many researches of acoustic behavior of micro-perforated plate have been studied theoretically and experimentally[2][3][4][5][6][7].

We have investigateed experimentally to make clear the relation between the vibration modes and the performance for the sound absorption of micro-perforated aluminium in detail[8]. Natural frequencies and vibration modes of the micro-perforated thin aluminium plate backed by cavity in the acoustic tube were observed by using the scanning laser Doppler vibrometer.

We find that both the special vibration mode and the phase difference of particle velocity and plate velocity affects the remarkable depression of sound absorption.

2. EXPERIMENTAL MEASURING PROCEDURE

2.1 APPRATUS AND INSTRUMENTATION

Figure1 shows the measuring system. The length of the acoustic tube is 1000mm. Inner diameter is 100mm. The loud speaker as acoustic driver, mounted at one end of the tube, is excited by the random noise signal. The transparent glass of 7mm thickness is set at another end. The perforated aluminium thin plate(MPP) is inserted and fixed between two flanges with 8 bolts and nuts. The depeth of the back space of the MPP is 30mm from the glass panel.

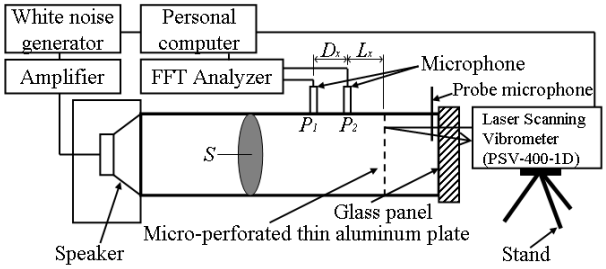

Figure 1. Block diagram of the measurement system forsound absortion coefficient and vibration behavior

Photo.1 Scanning laser vibrometer (left side) and specimen through glass panel (right side)

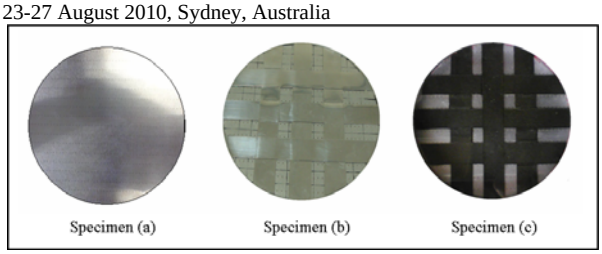

Photo.2 Three types of specimens

Table 1. Features of three specimens

Speci-men	*Thickness mm*	Orifce diameter mm	Open area ratio %	remarks
(a)	0.15	0.5	0.38	Added no damping 4.5g
(b)	0.15	0.5	0.38	Added damping and mass 10.4g
(c)	0.15	0.5	0.38	Added more damping and mass 18.9g

2.2 MEASURING PROCEDURE

Normal incidence absorption coefficient of MPPs was evaluated by using transfer function between the two microphone signals. Vibration displacement or velocity of almost all the area of plates is measured by using scanning laser Doppler vibrometer.

Three different types of MPPs, which are shown in Table1., were measured. Specimen(a) is only an aluminium MPP. In specimen(b), thin aluminium strips (thickness 0.1mm×width 13mm) are put on the adhesive tape(thickness 0.6mm) on the surface. In specimen(c), damping material (width13mm × thickness1.5mm)is put on the surface. Each of the weight of specimens (a), (b), (c) is 4.1g, 10.4g and 18.9g. Opening ratio and hole diameter is kept to be same for three spesimens.

3. ONE DIMENSIONAL THEORY OF SOUND FIELD IN ACOUSTIC TUBE WITH MPP

In the acoustic field shown in Fig.2, sound pressure p_1, p_2 and p_3, and volume velocity U_1, U_2 and U_3 are related by the following transfer matrices, if the MPP does not vibrate by acting vibration force of soundpressure.

$$\begin{Bmatrix} p_1 \\ U_1 \end{Bmatrix} = \begin{bmatrix} 1 & \Gamma/\sigma \\ 0 & 1 \end{bmatrix} \begin{Bmatrix} p_2 \\ U_2 \end{Bmatrix} \tag{1}$$

$$\begin{Bmatrix} p_2 \\ U_2 \end{Bmatrix} = \begin{bmatrix} \cos kl & j\dfrac{\rho c}{S}\sin kl \\ j\dfrac{S}{\rho c}\sin kl & \cos kl \end{bmatrix} \begin{Bmatrix} p_3 \\ U_3 \end{Bmatrix} \tag{2}$$

Therefore,

$$\begin{Bmatrix} p_1 \\ U_1 \end{Bmatrix} = \begin{bmatrix} 1 & \Gamma/\sigma \\ 0 & 1 \end{bmatrix} \begin{bmatrix} \cos kl & j\dfrac{\rho c}{S}\sin kl \\ j\dfrac{S}{\rho c}\sin kl & \cos kl \end{bmatrix} \begin{Bmatrix} p_3 \\ U_3 \end{Bmatrix}$$

$$= \begin{bmatrix} T_{11} & T_{12} \\ T_{21} & T_{22} \end{bmatrix} \begin{Bmatrix} p_3 \\ U_3 \end{Bmatrix} \tag{3}$$

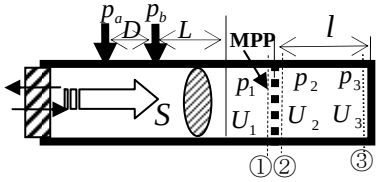

Figure 2. MPP backed by air space

Where[2][9], $\Gamma = j\omega M_A + R_A$, $R_A = 4R_V \dfrac{l+d}{d}$, $M_A = \rho l_e$

$R_V = 0.83\times10^{-2}\sqrt{f}$, $l_e = l + 0.8d\left(1 - 1.47\beta^{\frac{1}{2}} + 0.47\beta^{\frac{3}{2}}\right)$

d : orifice diameter, l : thickness of MPP, β : Open area ratio, ρ : density of air, c : sound speed

At the position ③ , $U_3 = 0$

Then, acoustic impedance Z_1 at position① is

$$Z_1 = p_1/U_1 = T_{11}/T_{21} \tag{4}$$

And specific acoustic impdance z_1 is $z_1 = Z_1/S$.

Normal incidence sound absorption coefficient α is calculated by using equation (5).

$$\alpha = 1 - \left|\frac{z_1 - \rho c}{z_1 + \rho c}\right| \tag{5}$$

On the other hand, acoustic impedance Z at arbitrary position is calculated by using equation (6), where H is the measured transfer function between two microphones.

$$Z = j\frac{\rho c}{S}\frac{-H\cdot\sin\{k(L+D)\} + \sin(kL)}{H\cdot\cos\{k(L+D)\} - \cos(kL)} \tag{6}$$

Where, $H = p_a/p_b$

4. ANALYSIS OF EXPERIMENTAL RESULTS

4.1 SOUND ABSORPTION COEFFICIENT

Figure 3 shows the comparison of sound absorption coefficient of specimen (a) between the calculation by the way described at section 3 and measured value applied by the two microphone technique. The MPP is supposed to be not vibrated in this calculation. These equations are proved to give good agreenent with meaeured data with thick MPP (3mm) of which vibration can be neglible. But we can recognize the difference between calculated and measured values in the region under about 650Hz. Main reason of this discrepancy supposed to be the vibration of the MPP. Especially local big depression of sound absorption coefficient around 560Hz, must be avoided, when we design sound absorption panels. So in this paper we focus this phenomena of big depression of sound absorption coefficient.

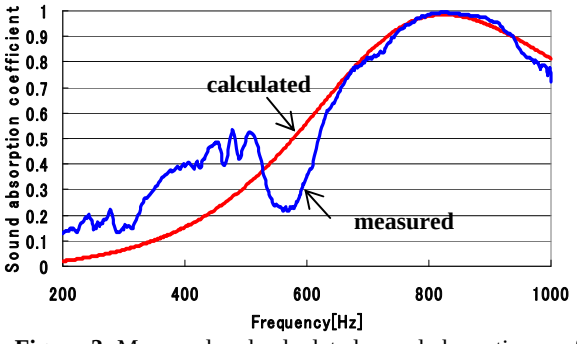

Figure 3. Measured and calculated sound absorption coefficient of specimen(a)

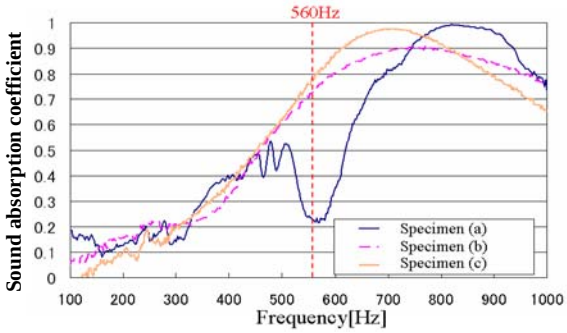

Figure 4. Comparison of measured sound absorption coefficient between specimen (a), (b), (c)

Figure 4 shows measured normal incidence sound absorption coefficient of specimen (a), (b) and (c). Specimen (a) has no additional damping. Specimen (b) and (c) have additional damping, mass and stifness shown in table 1. But open area ratio and hole diameter were kept same for thress specimens (a), (b) and (c) shown also in table1. We can recognize that the value of sound absorption coefficient around 560Hz is recovered in the case of specimen (b) and (c), and that the peak frequency of absorption coefficient is shifted to lower frequency. We can also recognize that the curve of specimen (b) around peak frequency is not so steeper than the curve of specimen (c) although the maximum value of sound absorption coefficient is lower than the case of specimen(c).

From Figure 3 and Figure 4 we can understand experimentally that sound absorption coefficient of the MPP is affected by its vibration.

4.2 MEASURED SOUNDPRESSURE

Figure 5 shows the spacial distribution of sound pressure and phase difference for the case of the specimen (a) to investigate sound wave near the MPP. Probe type microphone is traversed across on the cross section at 10mm distance from the suraface of MPP. The outer diameter of the probe is 5mm. We observed that there is almost no difference betwaeen measured data at 5 points of soundpressure level and phase difference in Figure 5.

We found that the behavior of acoustic wave is plane wave whithin 10mm near the MPP, though the MPP vibrates in many modes as shown in later section.

4.3 MEASURED VIBRATION OF MPP

Figure 6 shows mean value of vibration displacement over the almost all area of the MPP. We found that 5 peaks are observed in the frequnecy region of 200Hz to 850 Hz for the case of three specimens with and without adding damping and mass. These peaks are casued by acoustic resonces in the acoustic tube. Then we tried to normalize vibration displacement divided by sound pressure measured at 10 mm distance from the surface of the specimen.

Figure 7 shows the results of normalized vibration displacement for Figure 6 In Figure 7 we can recognize that 7 peaks in the data of specimen (a) and no distinguished steep peaks in the case of specimen (b) and (c). These peakes in the case of specimen (a) are natural frequencies of the perforated thin plate. We fond that damping is especially effective to extinguish these steep peaks. The value of normalized vibration velocity of specimen (b) and (c) are observed to be decreased remarkably in Figure 7. And each sound absorption coefficient of specimen (b) and (c) derived by two-microphone method shown in Figure 3 has same frequency characteristics as calculated ones in which perforated plate is assmued not to be moved in section 3. So we can understand that local depression of sound absorption coefficient around 560 Hz is casued by the vibration of the plate itself and that recovery of sound absorption coefficient around same frequency is caused by the reduction of vibration of it.

Figure 8 shows the comparison between sound absorption coefficient and mean value for vibration velocity of specimen (a) without damping. The frequency under 500 Hz at which steep peak of vibration velocity is observed coincides with local depression of sound absorption coefficient. But in the frequency region over 500 Hz we can find steep peaks of vibration velocity, but can not find local depression of sound absorption coefficient at that frequency. Big local depression of sound absorption coefficient is observed at 560 Hz in Figure 8, but peak frequency of the normalized vibration displacement is almost 600 Hz, and is slightly different from 560 Hz. The reason of this difference is because the normalized vibration velocity means averaged value of almost all the suraface area of the plate.

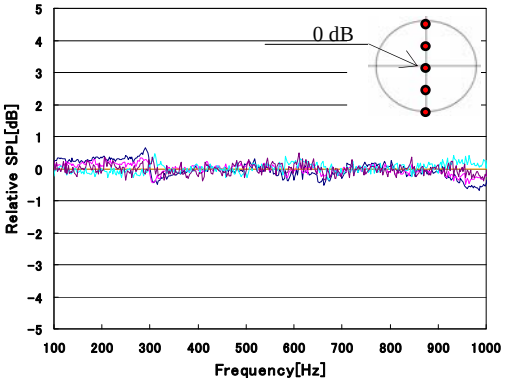

(a) Relative sound pressure level at 5 points

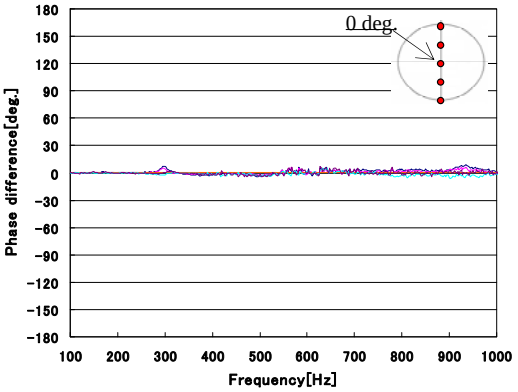

(b) Difference of phase angle between 5 points

Figure 5. Relative sound pressure levels and relative phase differences between 5 points at 10mm distance from MPP

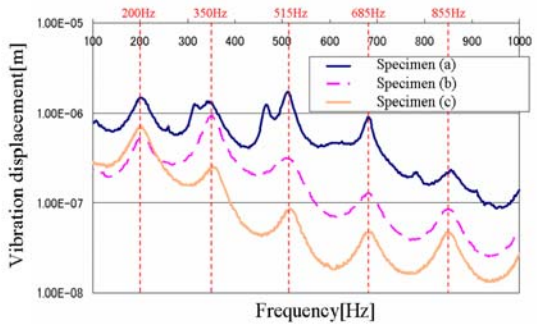

Figure 6. Mean value of measured vibration displacement of the MPP

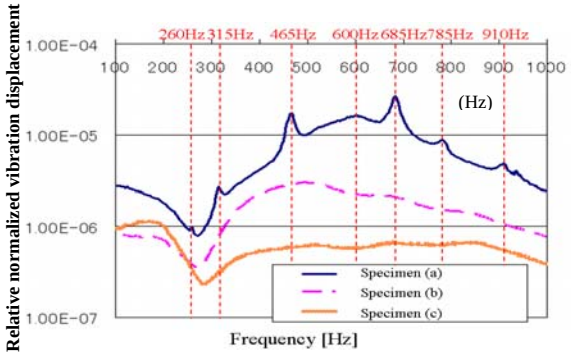

Figure 7. Mean value of measured vibration displacement normalized by sound pressure at 10mm distance from the MPP

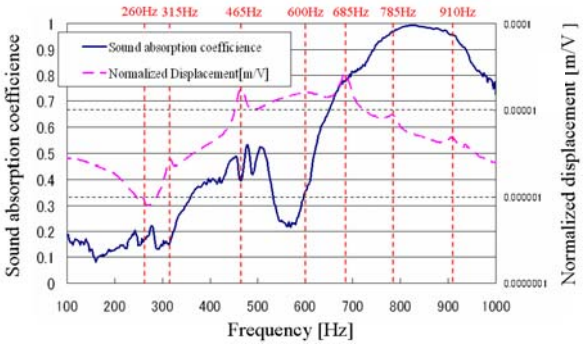

Figure 8. Sound absorption coefficient and normalized-vibrtion displacement by sound pressure of specimen (a)

Figure 9 shows normalized vibration velocity measured at the center of the specimen (a). In this case the frequency of 560Hz at which deep depression of sound absorbing coefficient is observed is the same frequency at which the frequency response of the vibration displacement shows peak. But this peak is not so steep but dull. It means that dumpimg effect for vibration is large in this frequency region.

It is found that natural vibration frequency of the MPP can be the frequency at which local depression of the sound absorption coefficient occures. But the degree of local depression of sound absorption coefficient is different. So we measured the vibration modes by using laser scanning vibrameter to investigate the relation between vibration modes and sound absorption.

Figure 10 shows vibration modes of the specimen (a). Left side figures show the results of experimental modal analysis. Right side figures show the results measured by the scanningvibrometer under the white noise excitation shown in Figure 1. In these figures the colors of red and green mean that phase of the vibration mode is opposite. And shade of colors means the amplitude of the vibration displacement. Lighter shade means larger amplitude of vibration. In Figure 10 resonant modes derived by both experimental modal analysis and laser scanning vibrometer agree well. Then it is recognized that natural mode is generated at the resonant frequency even under the white noise excitation in this acoustic tube. In Figure 10 the symbol (n, m) means the number of nodal cirles and nodal diameters respectively.

5. DISCUSSION

5.1 LOCAL DEPRESSION OF SOUND ABSORPTION COEFFICIENT AT (2,0) MODE

Local depression of sound absorption coefficient is remarkable at 560 Hz, at which vibration mode is (2,0) mode. This mode has no nodal daiameter, while (1,1) mode at 315 Hz

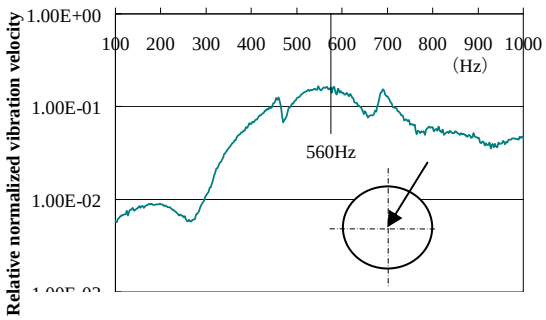

Figure 9 Normalized vibration velocity measured at the center of the specimen (a)

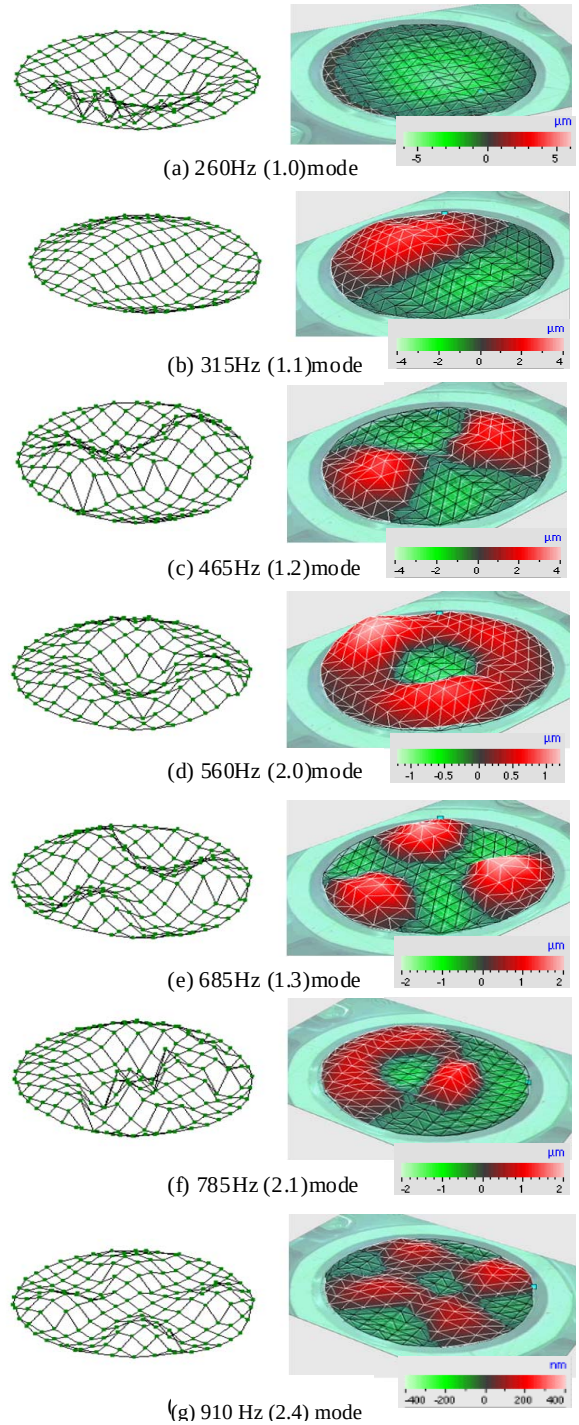

Figure 10. Natural frequencies and natural vibration modes of the specimen (a), (n, m) n ; nodal cirles, m ; nodal daiameters

and (1,2) mode at 465 Hz have nodal diameters at which local depression of sound absorption coefficient is not so large. We focused the relation between the vibration of this (2,0) mode and the volume velocity near the perforated plate.

We measured the acoustic impedance at 10 mm distance from the plate by using two microphone techniques.

The specific acoustic impedance Z_{10} at 10 mm distance from the plate was calculated by substituting the measured transfer function between two microphones for H in equation (6). As shown in Figure 5, sound pressure and phase angle on this cross section in the acoustic tube is observed to be almost same at each point. Then volume velocity U_{10} on this section can be derived from equation (7). Where p_{10} is the sound pressure at the center on this section at 10 mm distance from the plate.

$$U_{10} = \frac{1}{Z_{10}} p_{10} \tag{7}$$

The phase difference between vibration velocity V_i of the plate and volume velocity U_{10}, is derived by equation (8). Where V_i, p_{10} and Z_{10} are measured value.

$$\frac{V_i}{U_{10}} = V_i \frac{Z_{10}}{p_{10}} \tag{8}$$

Figure 11 shows the phase difference between volume velpocity and vibration velocity of the plate. As shown in Figure 10 (d), vibration of area 1 and 3 on the plate has same vibration phase, but this area has the phase difference of 180 degree for area 1, which means the area 1 and 3 vibrate oppositely to the area 1 of the plate. From this Figure 11, we can understand that the thin perforated plate of area 1 and 3 moves to the same direction of the volume velocity and that area 1 moves to the opposite direction of the movement of volume velocity around 560 Hz. But the area of region 2 is smaller than the area of region 1 and 3, so main area of the plate moves together with Volume velocity. In that case relative difference of particle velocity and vibration velocity becomes smaller, then energy transformation from acoustic energy to heat energy is decreased. This can be supposed to be as the reason why the remarkable depression of sound absorbing coefficient happens. Of course acoustic energy is transformed to heat energy effectively because of opposite direction of movement both vibration of the plate and volume velocity at area 2. But that area is smaller than the area of region 2 and 3. So the conversion from acoustic energy to heat energy on this area 2 is not predominant.

At other vibration modes nodal diameters are observed, we can recognize that almost same area vibrate oppositely in such mode, and we can understand that cancelation works so big depression of sound absorbing coefficient is not observed.

5.2 EFFECT OF ADDITIONAL DAMPING

As shown in Figure 4 damping material is effective to recover the local depression of sound absorption coefficient at 560 Hz. The change of vibration modes from (2,0) mode to (1,0) modes is observed for the case of specimen (b) and specimen (c) in Figure 12. The mode (2, 0) in specimen (a) is vanished in specimen(b) and specimen (c) by adding damping. The amplitude of specimen (b) and (c) are proved to be decreased remarkably as seen in Figure7. This is the main reason for recovery of depression of sound absorbing

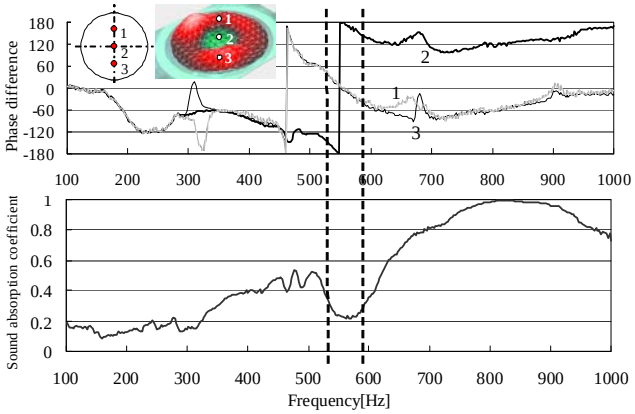

Figure 11. Comparison of sound absorption frequency char acteristics and phase difference between vibration velocity of the plate and the volume velocity

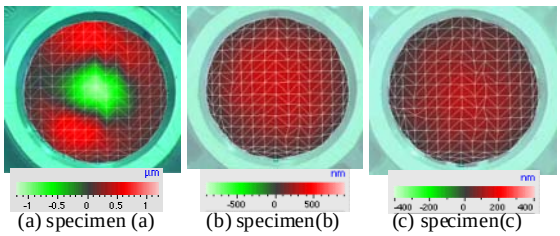

Figure 12. Vibration modes and special distribution of vibration amplitude for each specimen

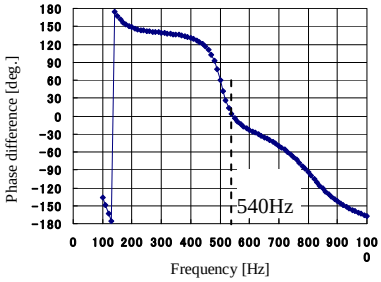

Figure 13. Computed difference of the phase between vibration displacement on the plate and sound pressure near the

coefficient. Of course increment of mass and stiffness of the damping material also contribute to decrease amplitude of vibration of the plate.

5.3 VALIDITY OF EXPERIMENTAL RESULTS BY USING NUMERCAL COMPUTATION

Computed difference of phase between vibration displacement of the plate and sound pressure near the plate is shown in Fig.13. Configuration and dimensions of the model for computation is same as described in section 2.1. We computed this model as vibro-acoustic coupled problem[10] by using boundary element method for acoustic field and finite element method for the MPP. This figure shows difference of phase angle becomes zero at 540 Hz as shown in figure11. It means that at this frequency the plate moves to the same direction as volume velocity moves. So we can recognize that

this result shown in figure 11 has the same tendency as computation analysis has.

5. CONCLUSIONS

Mainly experimental investigations of vibro- acoustic behavior for micro-perforated plate backed by an air cavity has been studied. The conclusions derived from this study can be summarized as follows.

(1) The amount of local depression of sound absorption coefficient in frequency characteristics depends on structural resonant modes of the plate.

(2) Local depression of sound absorption performance is remarkable in the case that resonant mode has no nodal diameter but omly nodal circles in the present experiment.

(3) Local depression of sound absorption performance is small and not so significant in the case that resonant mode has some nodal diameters and some nodal cirles.

(4) In the case that main area of the plate vibrates in phase with volum velocity, remarkable depression of sound absorption performance arises, because relative velocity between volume velocity and vibration of the plate is decreased.

(5) In the case that the vibration mode of the plate has some nodal diameters, cancellation of relative velocity in adjacent regions arises. So depression of sound absorption power is not significant.

(6) The reason of remarkable depression of sound absorption performance described at (4) is ascertained by computation result.

REFERENCES

1 T.Yamada, T. Tanaka, I. Yamagiwa, M.Horio, and H. Matsuda, “Development of the sound absorber panel composed of microperforated aluminum plate and foil” *Proceedings of the 17th Symposium of Environmental Engineering(JSME)*, 07-12, 105-108 (2007). (in Japanese)

2 U. Ingard, “On the theory and design of acoustic resonators” *J. Acoust. Soc. Am.*, Vol.25, No.61,1037-1062 (1953).

3 T. H. Melling, “The acoustic impedance of perforates at medium and high sound pressure levels” *J.Sound and Vibration*, Vol.29, No.1, 1-65 (1973).

4 D. Y. Maa, “Microperforated-panel wideband absorbers”, *Noise Control Engineering Journal*, Vol.29, No.3, 77-84 (1987)

5 K. Sakagami, M. Morimoto and W. Koike “A Numerical study of double leaf microperforated panel absorbers” *J. of Applied Acoustics*, Vol.67, No.7, 609-619 (2006).

6 M. Toyoda, M. Tanaka and D. Takahashi, ”Reduction of Acoustic radiation by perforated board and honeycomb layer systems” *J. of Applied Acoustics*, Vol.68, No.1, 71-85 (2007)

7 K. Tsugihashi, T.Tanaka and H.Ueda, ”Development of a technique to improve the sound insulation of double-leaf walls with air-space using microperforated sound absorbing plate”, *INTER-NOISE 2006 Proceedings* on CD-ROM, 457, 10pages(2006)

8 T.Kusakari, T.Tanaka and I.Yamagiwa, ”Analysis of vibro-acoustic behavior of micro-perforated thin aluminum plate for sound absorber” *Proceedings of the 19th Symposium of Environmental Engineering(JSME)*, No. 09-13, 123-126 (2009), (in Japanese)

9 C. Zwikker and C. W. Kosten, *Sound Absorbing Materials* (Elsevier Publishing, 1949).

10 K. Tsugihashi, T.Tanaka, ”Research on reduction of structure-borne sound using perforated plate (Numerical anlysis of sound radiation from perforated plate) *Proceedings of the 19th Symposium of Environmental Engineering(JSME)*, No.09-13, 74-77 (2009), (in Japanese)